

Investigation statistics of bipolar multilevel memristive mechanism and characterizations in a thin FeOx transition layer of TiN/SiO₂/FeOx/Fe structure

Yao-Feng Chang, Ting-Chang Chang, and Chun-Yen Chang

Citation: [Journal of Applied Physics](#) **110**, 053703 (2011); doi: 10.1063/1.3630119

View online: <http://dx.doi.org/10.1063/1.3630119>

View Table of Contents: <http://scitation.aip.org/content/aip/journal/jap/110/5?ver=pdfcov>

Published by the [AIP Publishing](#)

Articles you may be interested in

[Single- and bi-layer memristive devices with tunable properties using TiOx switching layers deposited by reactive sputtering](#)

[Appl. Phys. Lett.](#) **104**, 153505 (2014); 10.1063/1.4871709

[Observation of bias-dependent noise sources in a TiOx/TiOy bipolar resistive switching frame](#)

[Appl. Phys. Lett.](#) **104**, 083508 (2014); 10.1063/1.4865783

[In-operando and non-destructive analysis of the resistive switching in the Ti/HfO₂/TiN-based system by hard x-ray photoelectron spectroscopy](#)

[Appl. Phys. Lett.](#) **101**, 143501 (2012); 10.1063/1.4756897

[Publisher's Note: "Investigation statistics of bipolar multilevel memristive mechanism and characterizations in a thin FeOx transition layer of TiN/SiO₂/FeOx/Fe structure" \[J. Appl. Phys.110, 053703 \(2011\)\]](#)

[J. Appl. Phys.](#) **110**, 119904 (2011); 10.1063/1.3668129

[Conducting nanofilaments formed by oxygen vacancy migration in Ti/TiO₂/TiN/MgO memristive device](#)

[J. Appl. Phys.](#) **110**, 104511 (2011); 10.1063/1.3662922



Re-register for Table of Content Alerts

Create a profile.



Sign up today!



Investigation statistics of bipolar multilevel memristive mechanism and characterizations in a thin FeO_x transition layer of TiN/SiO₂/FeO_x/Fe structure

Yao-Feng Chang,¹ Ting-Chang Chang,^{2,3,b)} and Chun-Yen Chang^{1,a)}

¹Department of Electronics Engineering & Institute of Electronics, National Chiao Tung University, Hsinchu, 300, Taiwan

²Department of Physics, National Sun Yat-Sen University, Kaohsiung, 804, Taiwan

³Center for Nanoscience & Nanotechnology, National Sun Yat-Sen University, Kaohsiung, 804, Taiwan

(Received 2 July 2011; accepted 26 July 2011; published online 1 September 2011; publisher error corrected 31 October 2011)

We investigated multilevel resistance switching characteristics of the thin FeO_x transition layer in a TiN/SiO₂/FeO_x/Fe structure by controlling the current compliance and stopped voltage during the set and reset processes, respectively. It is observed that the resistive state could be easily tunable by controlling external electric conditions. The multilevel memristive mechanism was characterized by distinguishing the electrical behaviors statistically, inferring that the reset process is associated with the mobile-ion-assisted electrochemical redox. Moreover, the set process is also modeled by power dissipation behaviors. The presented mathematical and physical model provides a possibility to elucidate a universal mechanism for bipolar multilevel memristor. © 2011 American Institute of Physics. [doi:10.1063/1.3630119]

I. INTRODUCTION

Recently, resistance random access memory (RRAM) has become one of the most popular research areas for the next generation of non-volatile memory due to its superior characteristics of high operation speed (below 300 ps),¹ low power consumption,² and remarkable reliability.³ Also, RRAM has high capability to scale down its active size for future high-density production beyond NAND flash.^{4,5} In addition to improving storage density by device's architecture, specifically in reduction of the device size and 3D integration, another way to improve storage density is multilevel storage.^{6–8} Multilevel storage, which uses multiple distinguished high resistance states (HRS) and low resistance state (LRS) by controlling external electrical conditions, could be achieved. Wang *et al.* have reported the resistive switching mechanism and characterizations of multilevel memristor in Ti/Cu_xO/Pt structure by *I-V* characteristics.⁷ They proposed a possible model for their observation, which is that the increase of compliance current during the set process would induce more or stronger conducting filaments, and the increase of span voltage would result in driving more oxygen ions to rupture the conducting filaments more effectively. However, when they stated that the chemical redox reaction is the reason to cause the conducting filaments formation and rupture, they did not consider that the chemical reaction energy is conservative for the set and reset processes. Moreover, where does the chemical reaction energy come from? Although the multilevel resistive switching has been studied for many different materials^{7–10} and simulated in different

models,^{11–13} its complete mechanism has not yet been investigated by the statistics of electrical characterizations.

In our previous studies, a simple method to fabricate a thin FeO_x transition layer in TiN/SiO₂/FeO_x/Fe-contented electrode structure has been reported.^{14,15} The bipolar switching mechanism results from a redox reaction between the Fe₃O₄ phase (LRS) and Fe₂O₃ phase (HRS). Therefore, in this work, we studied the multilevel resistive switching mechanism and characterizations more detail during the set and reset processes by analyzing the statistics of the set and reset parameters. The aim of this study is to contribute three important points: (1) The resistive switching mechanism and characteristics were investigated by analyzing statistics of electrical results during the set and reset processes, specifically in controlling compliance current (CC) and stopped voltage (SV). (2) Based on the energy conservation concept in chemical redox reactions, we proposed the mobile-ion-assisted recovery during the reset process and the power dissipation model on series resistor during the set process, respectively. (3) We try to quantify the resistive switching characterizations by using statistical analyses. The presented mathematical and physical model provides a possibility and a concept to elucidate a universal mechanism for bipolar multilevel memristors.

II. EXPERIMENTAL PROCEDURES

A. Fabrication of resistive switching device

The detailed fabrication processes of the thin FeO_x transition layer device were described similarly in our previous study.^{14,15} A 50-nm-thick Fe layer was deposited on Pt/Ti/SiO₂/Si substrate by DC magnetron sputtering. Then, a ~50-nm-thick SiO₂ layer was deposited by plasma enhanced chemical vapor deposition system. Finally, a 50-nm-thick top electrode of TiN was sputtered and patterned in a square

^{a)}Author to whom correspondence should be addressed. Electronic mail: cyc@mail.nctu.edu.tw.

^{b)}Author to whom correspondence should be addressed. Electronic mail: tcchang@mail.phys.nsysu.edu.tw.

area with side length of 100 μm on the SiO_2 films. In order to improve devices resistance switching characteristics,¹⁵ a rapid thermal annealing treatment at 600 °C for 60 s was performed in argon ambient.

B. Characterization analysis

Keithley 4200 semiconductor characterization system is used to measure the current-voltage (I - V) characteristics 50 cycles per electrical conditions of the fabricated devices. For material analyses, transmission electron microscopy (TEM) and x-ray photoelectron spectroscopy (XPS) were carried out using a Philips Tecnai-20 Systems and Microlab 350 with a monochromatized Al $K\alpha$ x-rays source (1486.6 eV; 300 W), respectively. For surface topography analyses, scanning electron microscopy (SEM) was carried out using a HITACHI S-4000. The voltages were applied to the TiN top electrode and the Fe bottom electrode was grounded in 3 samples which always obtained consistent results. Have to mention that an electroforming process was required about 0.13 MV/cm for all of the annealed samples before the switching measurements.

It is noted that definitions of the “LRS Current”/“HRS Current” are the values of the current measured in the LRS/HRS at a voltage bias of 0.2 V. In addition, definitions of the “Set Current (I_{set})”/“Reset Current (I_{reset})” and “Set Voltage (V_{set})”/“Reset Voltage (V_{reset})” are the values of the current and voltage detected at the beginning of the resistance switching from a HRS/LRS to a LRS/HRS, respectively. The “Set Power (P_{set})”/“Reset Power (P_{reset})” is defined as the product of $I_{\text{set}}/I_{\text{reset}}$ and $V_{\text{set}}/V_{\text{reset}}$.

III. RESULTS AND DISCUSSION

A. Multilevel resistive switching effect

Figures 1(a) and 1(b) show that the continuous bipolar switching behaviors of the TiN/ SiO_2 /FeO_x/Fe structure with the 600 °C-60 s treated condition under a series of compliance current limitations, between 0.3 and 10 mA in a set process while the fixed stopped voltage is at 2.5 V, and, under a series of stopped voltage, between 1.25 and 2.75 V in a reset process while the fixed compliance current is at 5 mA, respectively. The stopped voltage is defined as the maximum value of negative sweeping voltage. It is obviously observed that the resistive state of the thin FeO_x material could be easily tunable by controlling external electric conditions. As can be observed in

Fig. 1(a), higher compliance current could provide higher total switching power to reach larger LRS current, meaning that stronger filaments in the resistive switching material can withstand much larger current.¹⁶ Of note, in order to recover the resistive state uniformly, a proper and fixed stopped voltage is selected under a series of compliance current limitations. Similarly, Fig. 1(b) suggested that the larger stopped voltage could result in more complete recover from LRS, which is determined under the same compliance current level, to HRS. The recovery process is reacted by critical localization Joule heating and assisted by the increasing electrical field to move mobile ion in electrochemical redox reactions (we will discuss afterward), so a higher resistive state could be reached to exhibit a smaller HRS current.

B. Statistics of electrical characterizations for CC effect

In order to investigate the multilevel memristive mechanism and characterizations in TiN/ SiO_2 /FeO_x/Fe structure, the electrical parameters, specifically in set/reset voltage, set/reset current and set/reset power, were extracted from Figs. 1(a) and 1(b) and were shown in Figs. 2 and 3, respectively. Figure 2 shows the statistics of the reset of voltage, current, and power as a function of compliance current. Most of the reset process parameters, such as reset voltage, reset current and reset power, increase with the compliance current except for the reset voltage at higher compliance current conditions of 8 and 10 mA [Fig. 2(a)]. The cause of the reset parameters increase was naturally suggested that a higher compliance current value results in the formation of stronger filaments, which need larger reset current [in the inset of Fig. 2(a)] as well as reset power [Fig. 2(b)] was required to rupture.¹⁶ Moreover, the sudden drop of the reset voltage at a higher compliance current condition was supposed that the reset process is dominated by localization Joule heating, which is limited by the filament’s thermal capability since its critical temperature is approximate the same to interrupt,¹¹ and results in lower reset voltage required.

C. Resistive switching mechanism for CC effect

In order to further explore the resistive switching mechanism in a thin FeO_x transition layer device, the relation between the average of reset current values and a series of

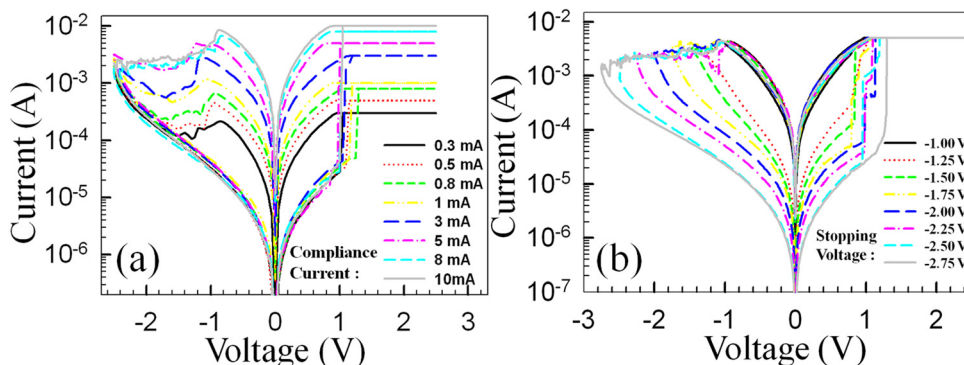


FIG. 1. (Color online) Continuous bipolar switching behaviors of the 600 °C-60 s treated TiN/ SiO_2 /FeO_x/Fe structure (a) under a series of compliance current in set process at fixed stopped voltage condition and (b) under a series of stopped voltage in reset process at fixed compliance current condition.

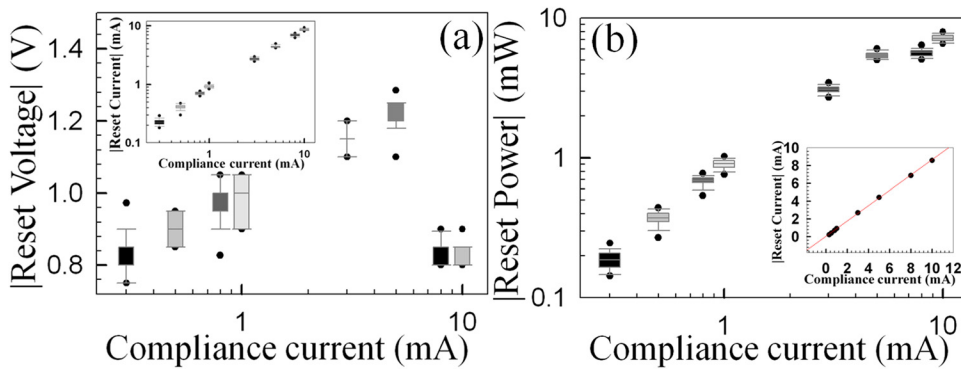


FIG. 2. (Color online) (a) Statistics plots of reset voltage and current (inset) as a function of compliance current. (b) Statistics plots of reset power as a function of compliance current. The inset shows the average reset current under a series of compliance current. The red dash fitting line shows a linear dependence between two currents.

compliance current limitations is shown in the inset of Fig. 2(b). Due to the lower reset current compared to its setup compliance current (the slope of linear fitting is 0.86), the reset process is based on the mobile-ion-assisted recovery by external electric field in electrochemical redox reactions¹⁷ rather than thermal-assisted switching mechanism,¹⁸ and this model is also consisted with the trend of reset voltage values increase with compliance current limitations. Therefore, it can be understood that the resistive switching mechanism in a thin FeO_x transition layer device is dependent mainly on the applied power which is comprehensive effect of reset voltage and reset current.

D. Statistics of electrical characterizations for SV effect

Figure 3 shows statistics of the set of voltage, current, and power as a function of stopped voltage. For set electrical parameters, it is observed that set voltage, which slightly increases with stopped voltage [in the inset of Fig. 3(a)], was in contrast to the set current, which decreases with increasing stopped voltage, as shown in Fig. 3(a). Moreover, in Fig. 3(b), the set power was calculated to slightly reduce and even saturate with increasing stopped voltage. Of note, although the statistics of set voltage have slight increased with stopped voltage, it did not mean that the switching thickness would change dramatically,¹⁹ where examined its cross-section image by TEM (not shown here). In addition, it is suggested that the thin FeO_x transition layers constitution would affect electrical characteristics,¹⁵ especially the distribution of oxygen vacancies and free oxygen species, are changed in different phases and recovered by different stopped voltage values.

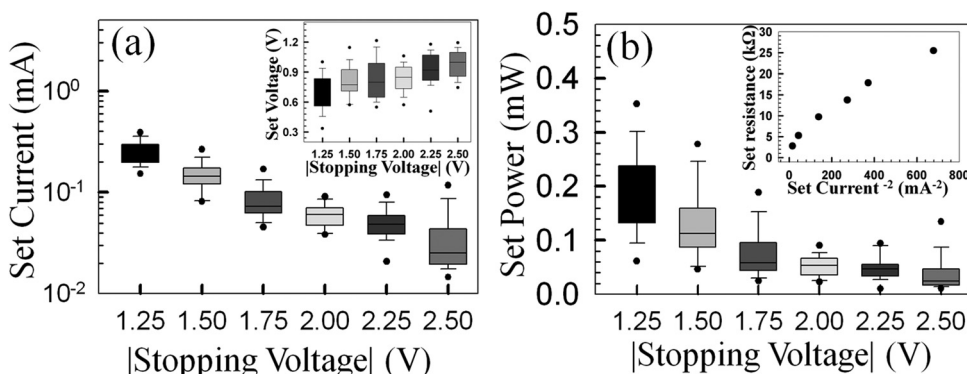


FIG. 3. (a) Statistics plots of set current and voltage (inset) as a function of stopped voltage. (b) Statistics plots of set power as a function of stopped voltage. The inset shows the relation between R_{set} and $1/I_{\text{set}}^2$ under a series of stopped voltage.

E. Resistive switching mechanism for SV effect

In order to elucidate the set power saturation phenomena with the increase of stopped voltage values, we proposed a power dissipation model on series resistor which means that the effective energy for “switchable” filaments is constant, also, the total resistance of the filaments could be separated by two parts: (1) the resistance of remained filaments (r_d), which is a nearly constant value after the forming process in the bulk, and (2) the resistance of “switchable” filaments (R_s), which can be tunable by external electrical power in a thin FeO_x transition layer. To prove our idea, the average of set resistance ($R_{\text{set}} \equiv V_{\text{set}}/I_{\text{set}}$) is assumptive equal to the sum of resistors ($R_{\text{set}} = r_d + R_s$), also, importantly, the boundary condition is determined by power-induced mechanism¹⁶ since the effective switching power ($I_{\text{set}}^2 R_s$) on “switchable” filaments under different stopped voltage conditions is equal to transform the electrochemical reaction from Fe_2O_3 phase (HRS) to Fe_3O_4 phase (LRS) in thin FeO_x transition layers. Therefore, these six algebra equations (different V_{set} and corresponding I_{set} results based on our setup measurement conditions) and one boundary condition can be solved by plotting the relation between R_{set} and $1/I_{\text{set}}^2$ under a series of stopped voltage, as shown in the inset of Fig. 3(b). The linearity (about 0.98) of these data shows that the proposed model is fitting our prediction what the transformation energy in redox reaction for a thin FeO_x transition layer device is constant, and also, it provides a possible mathematical quantification to physical model for multilevel memristive devices.²⁰

F. Material examination and analysis

As we mentioned previously, we did not find out the obviously different from the TEM analysis, specifically in

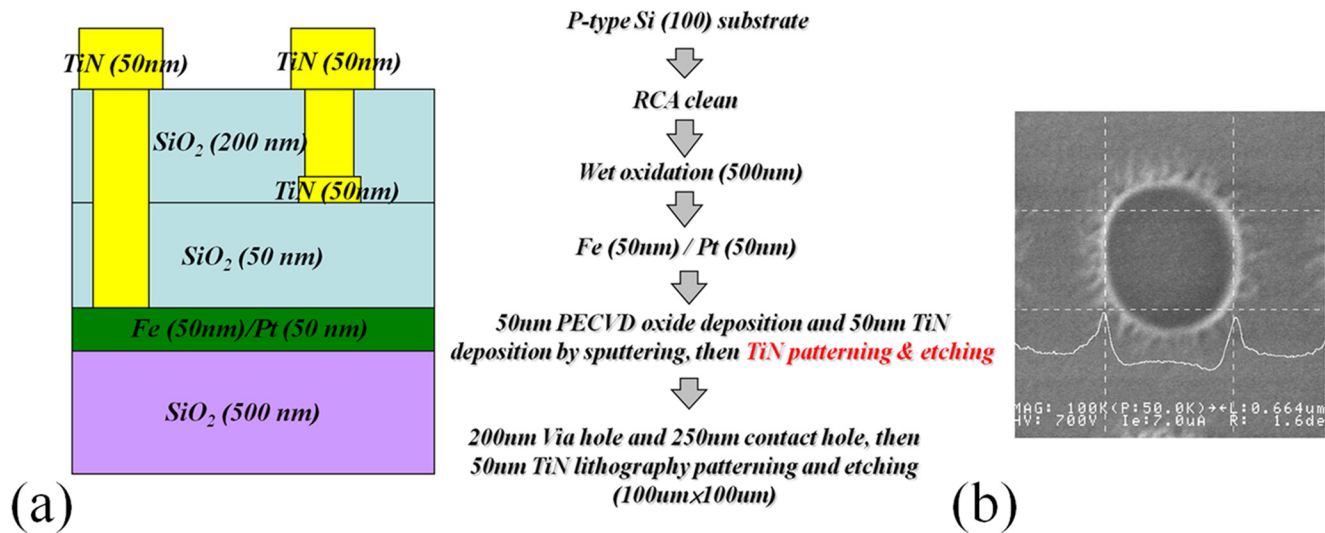


FIG. 4. (Color online) (a) Illustrations of the small size TiN/SiO₂/Fe/Pt structure and its process flows. (b) SEM images of the smallest via hole in our etching process.

the thickness of FeO_x transition layer after the electrical operation processes. Even we fabricated the small size device (maybe localized the resistive switching region), from $5 \times 5 \mu\text{m}$ to $0.6 \times 0.6 \mu\text{m}$, as shown in the Fig. 4, the obvious difference could not be observed by examining the cross-sectional TEM images before and after the electroforming process, and the set and reset processes. That is why we wonder that the thickness of a thin FeO_x layer did not change a lot during the electrical operation processes. Moreover, Lee *et al.* have studied the electromigration effects on the thickness of resistive switching materials. Their results show that if the thickness of resistive switching materials increases, the data dispersion of switching parameters would be deteriorated.¹⁹ However, in our measurement results, we did not observe these phenomena. On the other hand, the constitution of a thin FeO_x transition layer would affect the device's electrical characteristics and performances in our previous studies.¹⁵

In order to prove our hypothesis, we examined the chemical composition difference of the transition iron oxide layer at the localized region in our small size device, as shown in Fig. 5. Fe 2_{p3/2} XPS spectra of the FeO_x transition region of the TiN/SiO₂/FeO_x/Fe structure after a set process (in a LRS) and a reset process (in a HRS) were also analyzed under the

same Ar sputter etching time of 350 sec from top surface of PE-TEOS oxide (TiN top electrode was stripped). It is observed that compared to the HRS, the LRS shows a higher ratio of Fe₃O₄ composition (the ratio of Fe₃O₄ and Fe₂O₃), near the transition region. Therefore, it is further confirmed that the “set” and “reset” processes do change the valence state of iron oxide, which shows a chemical redox reaction of the transition layer during the “set” and “reset” operations.

G. Current transport examination and analysis

However, the intermediate states between LRS and HRS were hard to be observed by using XPS analysis. Therefore, we use electrical fitting analyses and define a linearity criterion of fitting curve strictly (over 99%) to accept the fitting results and then extract the electrical parameters, as shown in Figs. 6(a) and 6(b). In our previous studies,¹⁴ for HRS, the current transport behavior could be analyzed and separated into two parts: ohmic behavior at low electrical field and Frenkel-Poole emission at high electrical field. Of note, first, the ohmic transport behavior was fitting and selected the stopped voltage value by using our criterion [fitting by the formula (1)]. Second, similarly, the Frenkel-Poole transport behavior was continuous to fit from the previous stopped voltage and selected another stopped voltage value by our

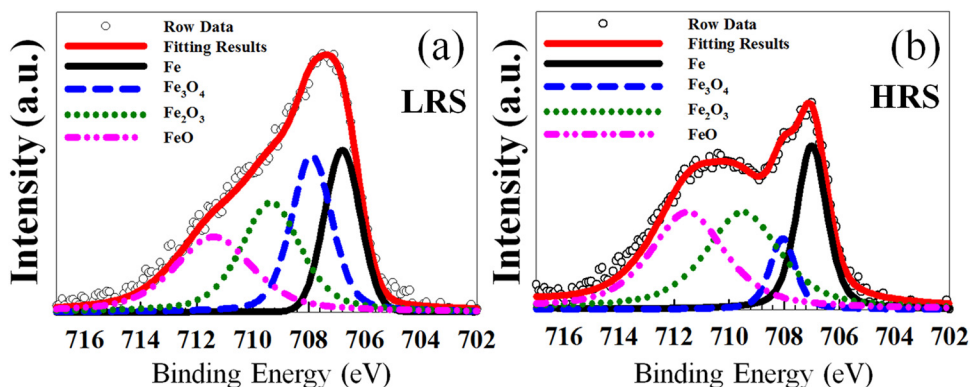


FIG. 5. (Color online) Fe 2_{p3/2} XPS spectra of the FeO_x transition region after (a) a set process (in a LRS) and (b) a reset process (in a HRS) under the same Ar sputter etching time of 350 sec from top surface of PE-TEOS oxide.

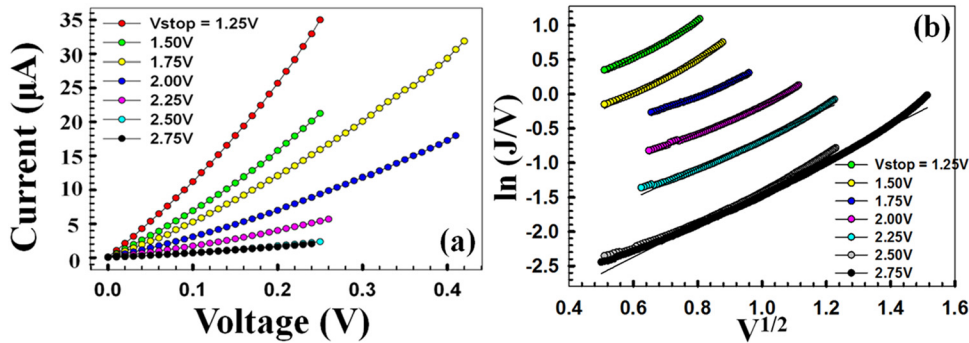


FIG. 6. (Color online) Linear fitting results for the TiN/SiO₂/FeO_x/Fe structure under a series of stopped voltage in the HRS region. (b) A plot of $\ln(I/V)$ vs $V^{1/2}$ under a series of stopped voltage in the HRS region. The linearity criterion of fitting curves is over 99%.

criterion [fitting by the formula (2)], as shown in Figs. 6 (a) and 6(b). Finally, we extracted the slope values of the P-F fitting results to get the relative permittivity when we defined the thickness of resistive “switchable” layer is 10 nm by using TEM and Auger electron spectroscopy analyses,¹⁴ as shown in Fig. 7.

$$\text{Ohmic conduction : } J = aV \exp\left(-\frac{c}{T}\right), \quad (1)$$

$$\begin{aligned} \text{Frenkel – Poole emission : } J \\ = BV \exp\left(\frac{-q(\phi_t - \sqrt{qV/\pi\epsilon_r\epsilon_0 d})}{kT}\right). \end{aligned} \quad (2)$$

In order to clarify the reset mechanism and our proposed idea logically, we analyze these data step by step. First, our main hypothesis is as follows: the thickness of the “switchable” layer would be fixed during the electrical operation. Based on this hypothesis, we could use the formula (2) to extract the relation between the relative permittivity and a series of stopped voltage. Theoretically, the values of the relative permittivity for Fe₂O₃, FeO, and Fe₃O₄ are 12, 14.2, and 20, respectively.²¹ In Fig. 7, we could separate the trend of these data by two parts: Above 1.75 V of the stopped voltage, the values of the relative permittivity could be fitting by using exponential function (linearity is over 99%) and their values are very close to the theoretical value when the thickness of the “switchable” layer is nearly constant. However,

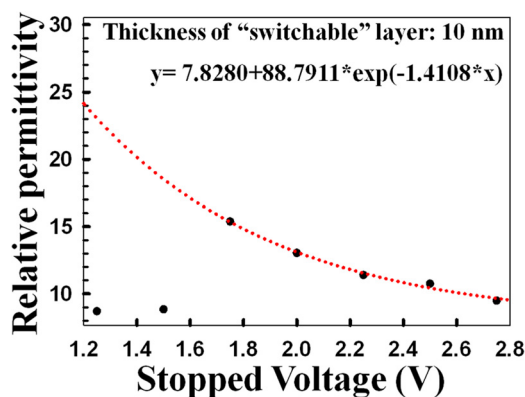


FIG. 7. (Color online) The relation between relative permittivity and a series of stopped voltage. The red dash fitting line shows an exponential function between 1.75V to 2.75V and extends for guiding the reader’s eye.

below 1.75 V of the stopped voltage, the value of the relative permittivity does depart from our hypothesis a lot. Therefore, our hypothesis, the thickness of the “switchable” layer is nearly constant, is wrong below 1.75 V of the stopped voltage. The XPS results show that a higher ratio of Fe₃O₄ composition (the ratio of Fe₃O₄ and Fe₂O₃) exists and it implies that the relative permittivity of the “less” HRS is higher than the “more” HRS (should be larger than 15). In other words, the reset process should be separated by two parts in our modified model:

First, the thickness of the “switchable” layer could be changed slightly (based on our fitting trend, at 1.25 V of the stopped voltage, the thickness of “switchable” layer would become 26.49 nm; at 1.50 V of the stopped voltage, the thickness of “switchable” layer would become 20.94 nm) because of the effectively joule heating, induced critical temperature at weak point, rupture the conducting filaments.^{11,17,18}

Second, the thickness of the “switchable” layer did not change extremely, but its composition is changed due to the mobile-ion-assisted recovery by external electric field in electrochemical redox reactions.¹⁷ These results are also consistent with our compliance current analyses.

H. Percolated filament’s properties for multilevel effect

Finally, Figs. 8(a) and 8(b) show that average and variation of the LRS current and HRS current under a series of compliance current and stopped voltage, individually. The average and variation of the LRS current would increase with the compliance current, as shown in Fig. 8(a). However, the average and variation of the HRS current would decrease with the increase of stopped voltage, as shown in Fig. 8(b). For Fig. 8(a), these phenomena suggest that the defects-induced percolated paths would be more plentiful to raise LRS current and more variable to form different percolated paths under higher compliance current conditions in set region. In contrast, for Fig. 8(b), the mobile-ion-assisted recovery process would interrupt and degrade the percolated paths more severely to lower HRS current and cause fewer disturbances under higher stopped voltage conditions in the reset region. The quantitative mathematical model for recover process of multilevel switching mechanism is still under study and will be provided by the reset process and low temperature dependence in the near future.

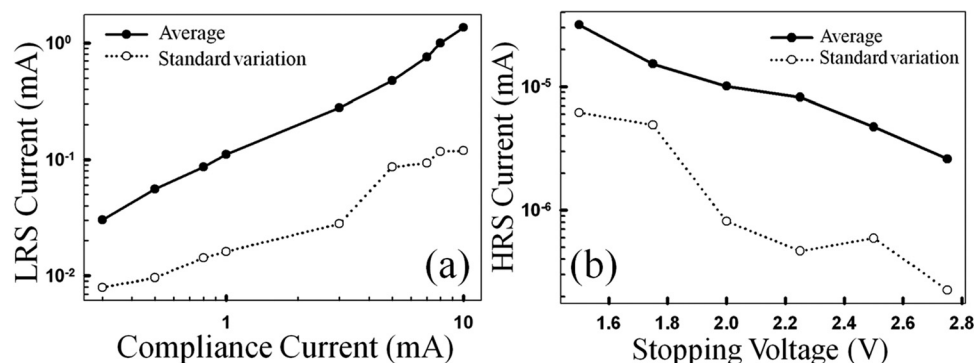


FIG. 8. (a) Average and standard variation of compliance current and (b) average and standard variation of HRS current under a series of stopped voltage.

IV. CONCLUSION

In conclusion, multilevel memristor of a thin FeO_x-transition layer in the TiN/SiO₂/FeO_x/Fe structure is demonstrated by controlling the compliance current and stopped voltage, respectively. Moreover, the resistive switching mechanism and its characterizations are investigated by analyzing the statistics of electrical results during the set and reset processes. Based on the concept of energy conservation in chemical redox reactions, we propose a power dissipation model on series resistor during the set process and the mobile-ion-assisted recovery during the reset process, respectively. In addition, the material phase properties and current transport behaviors in the TiN/SiO₂/FeO_x/Fe structure further confirm and modify the multilevel memristive mechanism in detail. These mathematical and physical models provide possible pictures to clarify a universal mechanism for bipolar multilevel memristor.

ACKNOWLEDGMENTS

This work was performed at National Nano Device Laboratory and was supported by the National Science Council of the Republic of China under Contract Nos. NSC-99-2120-M-110-001 and NSC 97-2112-M-110-009-MY3.

¹H. Y. Lee, Y. S. Chen, P. S. Chen, P. Y. Gu, Y. Y. Hsu, S. M. Wang, W. H. Liu, C. H. Tsai, S. S. Sheu, P. C. Chiang, W. P. Lin, C. H. Lin, W. S. Chen, F. T. Chen, C. H. Lien, and M. J. Tsai, *Tech. Dig. - Int. Electron Devices Meet.* 2010, 460.

²C. Schindler, M. Weides, M. N. Kozicki, and R. Waser, *Appl. Phys. Lett.* **92**, 122910 (2008).

³J. J. Yang, M.-X. Zhang, J. P. Strachan, F. Miao, M. D. Pickett, R. D. Kellley, G. M. Ribeiro, and R. S. Williams, *Appl. Phys. Lett.* **97**, 232102 (2010).

⁴M. J. Kim, I. G. Baek, Y. H. Ha, S. J. Baik, J. H. Kim, D. J. Seong, S. J. Kim, Y. H. Kwon, C. R. Lim, H. K. Park, D. Gilmer, P. Kirsch, R. Jammy,

Y. G. Shin, S. Choi, and C. Chung, *Tech. Dig. - Int. Electron Devices Meet.* 2010, 444.

⁵J. Lee, J. Shin, D. Lee, W. Lee, S. Jung, M. Jo, J. Park, K. P. Biju, S. Kim, S. Park, and H. Hwang, *Tech. Dig. - Int. Electron Devices Meet.* 2010, 452.

⁶H. Y. Lee, P. S. Chen, T. Y. Wu, Y. S. Chen, C. C. Wang, P. J. Tzeng, C. H. Lin, F. Chen, C. H. Lien, and M. J. Tsai, *Tech. Dig. - Int. Electron Devices Meet.* 2008, 297.

⁷S. Y. Wang, C. W. Huang, D. Y. Lee, T. Y. Tseng, and T. C. Chang, *J. Appl. Phys.* **108**, 114110 (2010).

⁸Y. Wang, Q. Liu, S. Long, W. Wang, Q. Wang, M. Zhang, S. Zhang, Y. Li, Q. Zuo, J. Yang, and M. Liu, *Nanotechnology* **21**, 045202 (2010).

⁹W. Guan, S. Long, Q. Liu, M. Liu, and W. Wang, *IEEE Electron Device Lett.* **29**, 434 (2008).

¹⁰C. Moreno, C. Munuera, S. Valencia, F. Kronast, X. Obradors, and C. Ocal, *Nano Lett.* **10**, 3828 (2010).

¹¹U. Russo, D. Ielmini, C. Cagli, and A. L. Lacaita, *IEEE Trans. Electron Devices* **56**, 193 (2009).

¹²U. Russo, D. Kamalanathan, D. Ielmini, A. L. Lacaita, and M. N. Kozicki, *IEEE Trans. Electron Devices* **56**, 1040 (2009).

¹³S. Yu, Y. Wu, and H. S. Philip Wong, *Appl. Phys. Lett.* **98**, 103514 (2011).

¹⁴L. W. Feng, C. Y. Chang, Y. F. Chang, W. R. Chen, S. Y. Wang, P. W. Chiang, and T. C. Chang, *Appl. Phys. Lett.* **96**, 052111 (2010).

¹⁵L. W. Feng, C. Y. Chang, Y. F. Chang, T. C. Chang, S. Y. Wang, S. C. Chen, C. C. Lin, S. C. Chen, and P. W. Chiang, *Appl. Phys. Lett.* **96**, 222108 (2010).

¹⁶C. Rohde, B. J. Choi, D. S. Jeong, S. Choi, J. S. Zhao, and C. S. Hwang, *Appl. Phys. Lett.* **86**, 262907 (2005).

¹⁷S. Yu and H. S. Philip Wong, *Tech. Dig. - Int. Electron Devices Meet.* 2010, 520.

¹⁸D. H. Kwon, K. M. Kim, J. H. Jang, J. M. Jeon, M. H. Lee, G. H. Kim, X. S. Li, G. S. Park, B. Lee, S. Han, M. Kim, and C. S. Hwang, *Nat. Nanotechnol.* **5**, 148 (2010).

¹⁹C. B. Lee, B. S. Kang, M. J. Lee, S. E. Ahn, G. Stefanovich, W. X. Xia-nyu, K. H. Kim, J. H. Hur, H. X. Yin, Y. Park, I. K. Yoo, J.-B. Park, and B. H. Park, *Appl. Phys. Lett.* **91**, 082104 (2007).

²⁰L. Goux, Y.-Y. Chen, L. Pantisano, X.-P. Wang, G. Groeseneken, M. Jurczak, and D. J. Wouters, *Electrochem. Solid-State Lett.* **13**, G54 (2010).

²¹K. F. Young and H. P. R. Frederikse, *J. Phys. Chem. Ref. Data* **2**, 313 (1973).